

CO investigation of $z = 0.4 - 1.5$ galaxies

A.-L. Melchior^{1,2} and F. Combes¹

¹ LERMA, Observatoire de Paris, LERMA, UMR8112, 61, avenue de l'Observatoire, Paris, F-75014, France
e-mail: A.L.Melchior@obspm.fr, Francoise.Combes@obspm.fr

² Université Pierre et Marie Curie-Paris 6, 4, Place Jussieu, F-75 252 Paris Cedex 05, France

Received ;date; / Accepted ;date;

ABSTRACT

We report on the results of an IRAM-30m search for CO emission lines in three galaxies at intermediate redshifts. The idea was to investigate the molecular content of galaxies bright in the infrared at $z = 0.4 - 1.5$, a redshift desert for molecular line studies, poorly investigated as of yet. We integrated 8-10h per source and did not succeed in detecting any of the sources. From our upper limits, we are able to constrain the molecular gas content in these systems to less than 4 to $8 \times 10^9 M_\odot$, assuming a CO-to-H₂ conversion factor ($\alpha = 0.8 M_\odot / (K \text{ km s}^{-1} \text{ pc}^2)$). We stress the current difficulty of selecting sources with a detectable molecular content, a problem that will be faced by the ALMA First Science projects.

Key words. infrared: galaxies – radio lines: galaxies – submillimetre – galaxies: general – methods: observational

1. Introduction

Our current knowledge of the molecular content of galaxies at $z > 0.4$ is currently limited to a fraction of the submillimetre bright objects (Solomon & Vanden Bout, 2005; Greve et al., 2005), usually selected on the basis of their strong infrared (IR) luminosity. The extent to which active galactic nuclei (AGN) contribute to these extreme infrared luminosity is currently a matter of debate. While the interpretation of the IR-radio correlation in terms of on-going star formation is commonly accepted (Condon et al., 1991; Condon, 1992; Yun et al., 2001), this explanation remains uncertain (e.g. Vlahakis et al., 2007). The evidence that, in the strongest infrared sources, a significant fraction of the infrared luminosity is due to AGN (Genzel & Cesarsky, 2000; Alexander et al., 2005) further complicates the interpretation of this correlation. Farrah et al. (2003) have shown a correlation of the AGN and starburst luminosities over a wide range of IR luminosities. The recent detection of a molecular torus in Arp 220 (Downes & Eckart, 2007) demonstrates that the true source of at least part of its infrared luminosity is due to a black hole accretion disc, while this galaxy was considered as a prototypical starburst. Hence, there is the possibility that the infrared luminosity is not a good tracer of star formation activity, which is quite troublesome because this is nevertheless the most reliable and easy tracer used so far (at least unbiased by dust extinction).

In this complex context, the detection of molecular gas emission is essential to get information about the mass and dynamics of these galaxies, and to confirm the huge star formation rates ($750\text{--}1000 M_\odot \text{ yr}^{-1}$) usually derived for (sub)millimetre galaxies. Ultimately, this will contribute to further constrain the scenario of hierarchical galaxy formation and evolution. However, the current sensitivities are relatively low and require configurations with huge amount of gas. Different types of samples have been investigated so far, with various success. On the one hand, Evans et al. (2006), in their study of molecular

gas in quasi-stellar objects $z < 0.15$, found a low CO to infrared luminosity ratio, suggesting that the infrared luminosities of these QSO might be dominated by the AGN component. Saripalli & Mack (2007) failed to detect any molecular gas in restarting radio galaxies at $z < 0.15$. On the other hand, for the high- z galaxies with a CO detection, starbursts and AGN do not exhibit significant differences in their molecular gas content (Solomon & Vanden Bout, 2005; Greve et al., 2005). However, there is a clear difference in the CO line widths, a factor of 2.3 narrower in velocity in QSO host galaxies with respect to submillimetre galaxies, while powerful radio galaxies fall in between (Greve et al., 2005; Carilli & Wang, 2006). The origin of this effect is not yet clear: it could be due to a systematic in the orientation of the QSO, but the possibility of merger signatures in submillimetre galaxies is not excluded.

The redshift range $z = 0.4 - 1.5$ corresponds to a key period of the star formation history of the Universe: the end of the Star Formation plateau (e.g. Madau et al., 1998; Dahlen et al., 2007) converging to the nearby galaxy population. This range has been poorly investigated in CO so far due to the lack of appropriate detectors and is known as a redshift desert for molecular studies. This desert is due to the presence of atmospheric lines (O₂), which prevent the detection of CO(1-0) below 81 GHz. (A similar situation was observed in optical spectroscopy for galaxies with $z = 1.5 - 2.5$ (Steidel et al., 2004).) However, while most $z > 1.5$ sources detected in CO are magnified, the lower redshift range is relatively more favourable to CO detection because there is no negative K-correction for CO (Combes et al., 1999).

In this paper, we discuss the search for CO emission lines in three galaxies at intermediate redshifts, in order to investigate the molecular gas content of galaxies bright in the infrared at $z = 0.4 - 1.5$.

Throughout this paper, we adopt a flat cosmology, with $\Omega_m = 0.24$, $\Omega_\Lambda = 0.76$ and $H_0 = 73 \text{ km s}^{-1} \text{ Mpc}^{-1}$ (Spergel et al., 2007).

Table 1. Characteristics of the galaxies studied in this paper. Listed from left to right are the names of the sources, their J2000.0 positions, infrared luminosities, rest-frame B-band luminosities, galaxy types, redshifts, and luminosity distances. The appropriate references for the listed infrared luminosities and redshifts are given in the rightmost column. The values of L_B^{rest} are from Weiner et al. (2005) for the CFRS sources, and computed with the 2MASS J-band flux for NGP9 F268-0341339.

Source	RA (J2000)	DEC (J2000)	L_{IR} ($10^{11} L_{\odot}$)	L_B^{rest} ($10^{11} L_{\odot}$) [L_B^*] ^a	Type	Redshift	D_L (Gpc)	Ref.
CFRS 14.1329	14:17:34.8	+52:27:52.0	1.3 ± 0.2^b	0.04 [2]	LIRG	0.375	1.96	1, 2
CFRS 14.1157	14:17:41.9	+52:28:24.0	67 ± 4	0.53 [25]	ULIRG	1.149	7.84	3, 2
NGP9 F268-0341339	12:28:47.4	+37:06:12.3	—	6.9 [328]	QSO, synch.	1.515	11.12	4

1: Zheng et al. (2004); 2: Hammer et al. (1995); 3: LeFloch, private communication; 4: Snellen et al. (2002).

^a $L_B^* = 2.1 \times 10^9 L_{\odot}$ (Marzke et al., 1998). ^b Flores et al. (1999) initially estimated $L_{\text{IR}} = 6.3 \pm 0.3 \times 10^{11} L_{\odot}$.

2. Source selection

We initially defined a sample of star-forming galaxies from the Canada France Redshift Survey (CFRS, Lilly et al., 1995). We chose galaxies with an infrared-based star formation tracer indicating a SFR larger than $100 M_{\odot} \text{ yr}^{-1}$ (Flores et al., 1999; Hammer et al., 1995). We also considered a subset of strong radio-sources from the FIRST survey, for which redshifts were available. In total, three sources were observed: CFRS 14.1329 and CFRS 14.1157 (two sources from the CFRS with ISO and VLA detections) and NGP9 F268-0341339 (a flat spectrum radio galaxy selected from the FIRST survey).

The infrared luminosities¹, available for the CFRS sources (Zheng et al., 2004, Le Floch, priv. comm.), are provided in Table 1 together with the other (updated) known characteristics of these galaxies. Appendices A and B provide more details about CFRS 14.1329 and NGP9 F268-0341339.

3. CO Observations and reduction of the data

We observed at IRAM-30m in May 2000 CO lines in the following galaxies: CFRS 14.1329, CFRS 14.1157 and NGP9 F268-0341339. Table 1 displays their main properties.

Wobbler-switching mode was used, with reference positions offset in azimuth by $90''$ for CFRS 14.1329 and CFRS 14.1157 and $200''$ for NGP9 F268-0341339. At 1 and 3 mm, we used respectively 1 MHz filterbank and the autocorrelator (1.25 MHz/channel) with bandwidths of 512 and 640 MHz.

The reduction was performed by the IRAM GILDAS software². For each line, the spectra have been added and a polynomial of order 1 has been fitted and subtracted.

3.1. CFRS 14.1329

We searched for the CO(1-0) line at 83.83 GHz and the CO(3-2) line at 251.49 GHz, relying on the spectroscopic redshift $z = 0.375$. At these frequencies, the telescope's half-power beam widths are respectively $29''$ and $9.1''$. We integrated 8.5 h on this source, with typical system temperatures of 203 K and 1117 K (on the T_A^* scale). The observing conditions were not very stable (wind). We calibrated the spectra using the standard S/T_A^* factors: 6.0 and 9.2 Jy K^{-1} . As displayed in Fig. 1, we do not detect any line at the 1.7 and 12.0 mJy (rms) level.

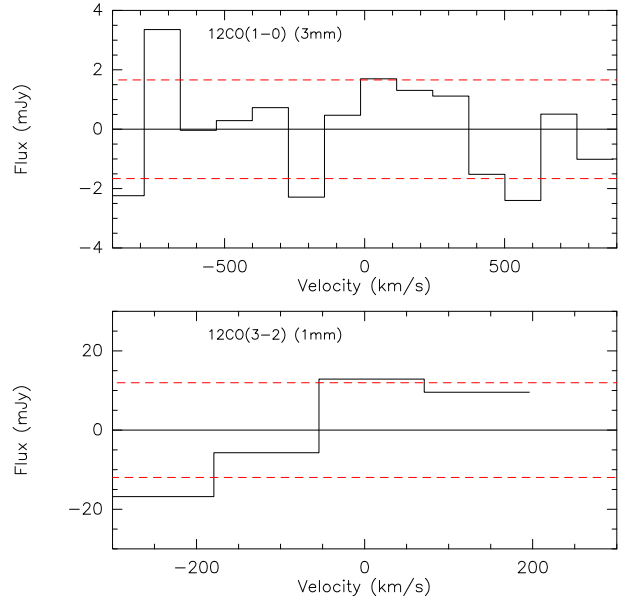


Fig. 1. Non-detection of the CO(1-0) and CO(3-2) lines searched in CFRS 14.1329 at IRAM-30m (2000 May 3-4) at the spectroscopic redshift ($z = 0.375$) of the host galaxy. The displayed channel separations are 128.7 km s^{-1} (top panel) and 125.2 km s^{-1} (bottom panel). The dashed (red) lines indicate the 1-sigma levels reached for this 8.5 h integration.

3.2. CFRS 14.1157

We searched for the CO(2-1) line at 107.28 GHz and the CO(4-3) line at 214.54 GHz, relying on the spectroscopic redshift $z = 1.149$. At these frequencies, the telescope's half-power beam widths are respectively $22''$ and $12''$. We integrated 7.8 h on this source, with typical system temperatures of 147.8 K and 324.1 K (on the T_A^* scale). We calibrate the spectra using the standard S/T_A^* factors: 6.3 and 7.9 Jy K^{-1} . As displayed in Fig. 2, we do not detect any line at the 1.8 and 3.7 mJy (rms) level. There is obviously some structures in the baseline at 107.28 GHz. However, this 1σ bump is too weak to claim any detection and is most probably due to variable baselines, so we do not apply any correction.

3.3. NGP9 F268-0341339

We searched for the CO(2-1) line at 91.670 GHz and the CO(5-4) line at 229.130 GHz, relying on the spectroscopic redshift $z = 1.515$. At these frequencies, the telescope's half-power beam widths are respectively $27''$ and $11''$. We integrated 10.3 h on this source, with typical system temperatures of 147 K and 495 K (on the T_A^* scale). The observing conditions were not very stable. We

¹ Please note that throughout the paper, L_{IR} is defined as the integral of the flux between 8 and $1000 \mu\text{m}$, while $\text{SFR} = 1.71 \times 10^{-10} \frac{L_{\text{IR}}}{L_{\odot}}$ (Kennicutt, 1998). Following Elbaz et al. (2002), we took $L_{\text{IR}} = (1.91 \pm 0.17) \times L_{\text{FIR}}$, where L_{FIR} is defined in the range $40\text{--}120 \mu\text{m}$.

² <http://www.iram.fr/IRAMFR/GILDAS>

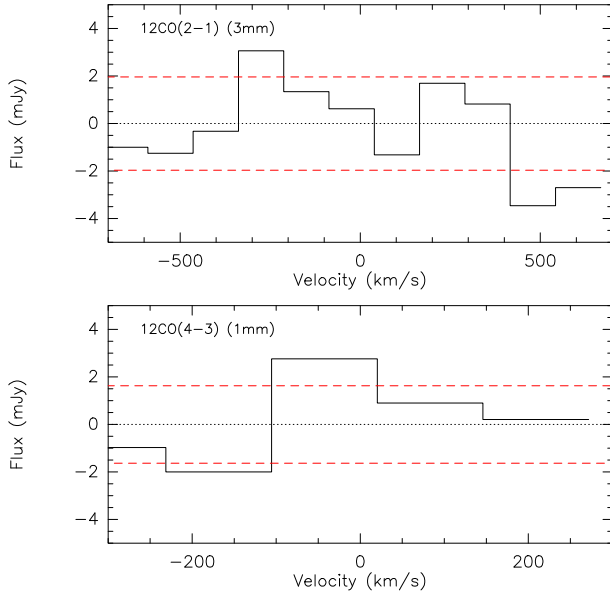


Fig. 2. Non-detection of the CO(1-0) and CO(3-2) lines searched in CFRS 14.1157 at IRAM-30m (2000 May 4-5) at the spectroscopic redshift ($z = 1.149$) of the host galaxy. The displayed channel separations are 125.8 km s^{-1} (top and bottom panel). The dashed (red) lines indicate the 1-sigma levels reached for this 7.8 h integration.

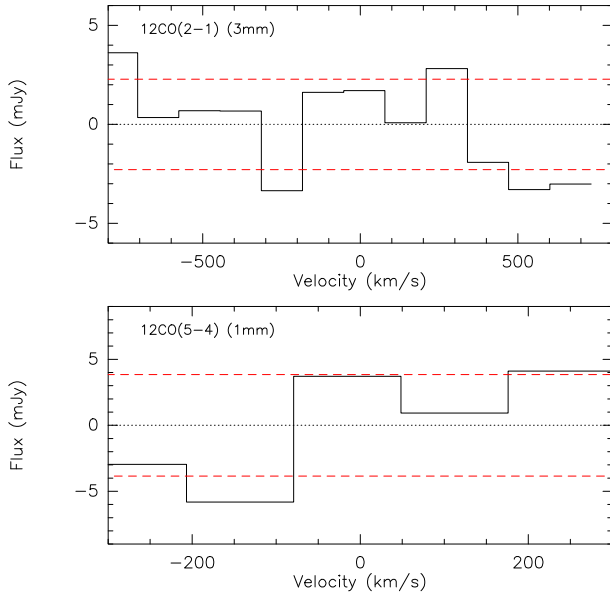


Fig. 3. Non-detection of the CO(2-1) and CO(5-4) lines searched in NGP9 F268-0341339 at IRAM-30m (2000 May 6-9) at the spectroscopic redshift ($z = 1.515$) of the galaxy. The displayed channel separations are 130.8 km s^{-1} (top panel) and 127.6 km s^{-1} (bottom panel). The dashed (red) lines indicate the 1-sigma levels reached for this 10.35 h integration.

calibrated the spectra using the standard S/T_A^* factors: 6.1 and 8.6 Jy K^{-1} . As displayed in Fig. 3, we do not detect any line at the 2.3 and 3.8 mJy (rms) level.

4. Analysis

Given the secure spectroscopic optical redshift and the large bandwidth at 3 mm, we do not expect a large velocity shift, which could explain this missing CO emission. Very few galaxies (usually at $z > 3$) present a CO-line width (FWHM) larger than 1000 km s^{-1} . We would have detected a signal at 3 mm given our reduction procedure.

Following Seaquist et al. (1995), we calculate upper limits on the velocity-integrated line fluxes using:

$$S_{CO}\Delta v = 3 \sqrt{\Delta v_{ch}/\Delta v} \sigma_{ch} \Delta v \quad (1)$$

where σ_{ch} is the channel-to-channel dispersion (rms) computed in Jy for a given channel width Δv_{ch} (in km s^{-1}) and Δv is the (expected) line width in km s^{-1} . For the latter, we assumed a value of 300 km s^{-1} . These upper limits are calculated from the final, binned spectra shown in Fig. 1, 2 and 3.

From the upper limits on the velocity-integrated line fluxes, the corresponding constraints on CO line luminosities are computed as:

$$L'_{CO} = 3.25 \cdot 10^7 S_{CO} \Delta v \frac{D_L^2}{v_{rest}^2 (1+z)} \quad (2)$$

where L'_{CO} is the CO-line luminosity expressed in $\text{K km s}^{-1} \text{ pc}^2$, v_{rest} is the rest frequency of the line in GHz, and D_L the luminosity distance in Mpc (Wright, 2006).

We expect that the CO flux (S_{CO}) is increasing as $\sim v_{rest}^2$ for the first CO lines, for a given H_2 mass, as derived for starbursts by Combes, Maoli & Omont (1999). The ratios $L'_{CO}(J = 2-1)/L'_{CO}(J = 1-0)$, $L'_{CO}(J = 3-2)/L'_{CO}(J = 1-0)$, $L'_{CO}(J = 4-3)/L'_{CO}(J = 1-0)$ and $L'_{CO}(J = 5-4)/L'_{CO}(J = 1-0)$ are thus taken to be equal to 1. This assumes that the lines are thermalised at high temperature and optically thick. For objects like quiescent nearby galaxies our upper values should be multiplied by a factor up to 1.1 (Braine & Combes, 1992), 1.6 (Devereux et al., 1994), 2.2 and 4.8 (Papadopoulos et al., 2000). However, our galaxies are probably starbursts not representative of nearby sources, so we do not apply any correction.

Figure 4 displays the upper limits derived from our observations on L'_{CO} , compared to previous detections of submillimetre galaxies detected in CO (Greve et al., 2005; Yao et al., 2003; Solomon et al., 1997; Sanders et al., 1991). These limits can be compared to the IRAM-30m best detection limits. They are displayed in Fig. 4 and correspond to $S_{CO}\Delta v = 1 \text{ Jy km s}^{-1}$ for various CO lines achieved at IRAM-30m. They illustrate the coverage of CO(1-0) measurements and the complementarity of the other CO transition lines.

Fig. 5 exhibits the correlation between the infrared and CO luminosities. The upper limits are consistent with the IR-CO correlation given its significant scatter. The two arrows provided for CFRS 14.1157 correspond to the total IR luminosity and to the sole contribution of the starburst, as discussed in Sect. 5.

5. Discussion

The non-CO detections discussed here reveal the difficulties of selecting favourable candidates. The scatter of the correlation between the IR and CO luminosities (see Fig. 5) is large and probably linked to the fact that the IR luminosities does not trace the star formation activity only. In addition, it is difficult to obtain IR luminosities, given the lack of all-sky survey since IRAS. The only solution has been here to rely on IR luminosities

Table 2. Upper limits computed for the two CO-lines studied in each object (IRAM-30m observations). We provide 3σ upper limits on the line integrated intensity $S_{CO}\Delta v$ and the CO line luminosity L'_{CO} , assuming a line width of 300 km s^{-1} .

Lines	CFRS 14.1329	Lines	CFRS 14.1157	Lines	NGP9 F268-0341339
Upper limits on $S_{CO}\Delta v$ (Jy km s^{-1})					
CO(1-0)	1.0	CO(2-1)	1.05	CO(2-1)	1.4
CO(3-2)	7.0	CO(4-3)	2.16	CO(5-4)	2.2
Raw upper limits on L'_{CO} ($10^9 \text{ K km s}^{-1} \text{ pc}^2$)					
CO(1-0)	6.9	CO(2-1)	18.4	CO(2-1)	41.1
CO(3-2)	5.3	CO(4-3)	9.4	CO(5-4)	10.7

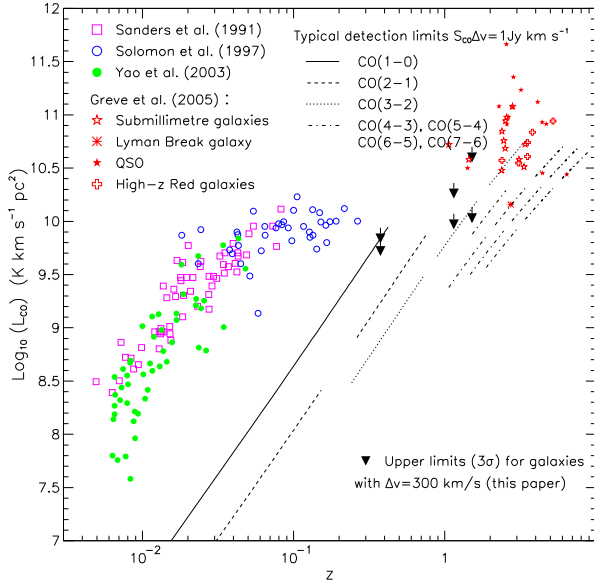


Fig. 4. CO-line luminosities L'_{CO} as a function of redshift. Upper limits (based on $\Delta v = 300 \text{ km s}^{-1}$) measured here for the studied galaxies are superimposed on previous measurements from Greve et al. (2005), Yao et al. (2003), Solomon et al. (1997) and Sanders, Scoville & Soifer (1991). The two upper limits (3σ), displayed for each source, correspond to the two measurements performed at 1 and 3 mm. None of the CO-line luminosities has been corrected for gravitational lensing. The curves correspond to an integrated flux $S_{CO}\Delta v = 1 \text{ Jy km s}^{-1}$.

derived from shorter wavelength measurements (namely $15\mu\text{m}$ Flores et al., 1999; Zheng et al., 2004).

The lack of CO detections towards CFRS 14.1329 and NGP9 F268-0341339 is probably due to the fact that they are not as good candidates as we initially thought. As explained in Appendix A, CFRS 14.1329 had been selected on the basis of a favourable L_{IR} luminosity (Flores et al., 1999), which was subsequently revised (Zheng et al., 2004). We also discussed in Appendix B that NGP9 F268-0341339 is behind a foreground galaxy at $z = 0.138$ with $\text{SFR} \sim 95 M_{\odot} \text{ yr}^{-1}$.

From our upper limits on the CO(1-0) and CO(3-2) luminosities, we estimate that the molecular gas content³ of CFRS 14.1329 is smaller than $5.5 \times 10^9 M_{\odot}$ and $4.2 \times 10^9 M_{\odot}$, assuming a molecular gas mass to CO luminosity ratio $\alpha = 0.8 M_{\odot} (\text{K km s}^{-1} \text{ pc}^2)^{-1}$, typical of ultraluminous infrared galaxies (ULIRG) (e.g. Solomon & Vanden Bout, 2005). These total molecular gas masses are consistent with the gas content of local normal spiral galaxies (Gao & Solomon, 2004), while the in-

³ Following Solomon & Vanden Bout (2005), our molecular gas content estimates account for the He mass.

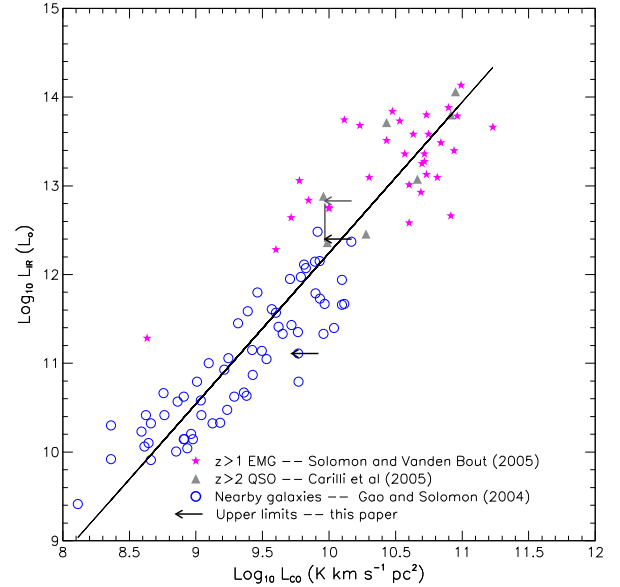


Fig. 5. The infrared and CO luminosities of nearby galaxies (Gao & Solomon, 2004), ($z > 2$) QSO (Corilli et al., 2005) and ($z > 1$) Molecular Emission Line Galaxies (Solomon & Vanden Bout, 2005) are compared to the 1-mm upper limits obtained for the CFRS sources studied in this paper. For CFRS 14.1157, the total IR luminosity and the starburst contribution estimated by Le Floc'h et al. (2007) are considered. The line corresponds to the fit obtained by Solomon & Vanden Bout (2005). The high- z data are corrected for gravitational lensing magnification when the factor is known.

frared luminosity (derived from $15\mu\text{m}$ data) was suggesting a luminous infrared galaxy (LIRG). Hence, the value of α is uncertain and probably underestimated. For the more distant galaxy NGP9 F268-0341339, the limits are less stringent and it is still compatible with an (U)LIRG. With the same assumptions, the molecular mass is smaller than $33 \times 10^9 M_{\odot}$ and $8.6 \times 10^9 M_{\odot}$ according to our upper limits on the CO(2-1) and CO(5-4) luminosities. The luminosities derived from higher CO line transitions are more stringent than those derived from the lower ones as we assumed that the lines were optically thick (see also Sect. 4).

In contrast, CFRS 14.1157 was a very favourable candidate that has remained as such. Zheng et al. (2004) estimated $L_{IR} = 178.6 \times 10^{11} L_{\odot}$ ($\text{SFR} \sim 3054 M_{\odot} \text{ yr}^{-1}$), relying on the IR- $15\mu\text{m}$ luminosities correlation measured by Elbaz et al. (2002). Le Floc'h et al. (2007) published a panchromatic spectral energy distribution of this galaxy with a very good wavelength cover-

age. They derived a direct estimate⁴ of the infrared luminosity computed over the range $8-1000\mu\text{m}$: $L_{\text{IR}} = 67 \pm 4 \times 10^{11} L_{\odot}$, which would correspond to $\text{SFR} \sim 1150 M_{\odot} \text{yr}^{-1}$. However, Le Floc'h et al. (2007) have estimated that 67.2% percent of the infrared flux is due to the AGN component. Accordingly, the SFR is probably of order $375 M_{\odot} \text{yr}^{-1}$.

From our upper limits on the CO(2-1) and CO(4-3) luminosities of CFRS 14.1157, we find that the molecular gas content of this galaxy is smaller than $15 \times 10^9 M_{\odot}$ and $7.5 \times 10^9 M_{\odot}$ (with $\alpha = 0.8 M_{\odot} (\text{K km s}^{-1} \text{pc}^2)^{-1}$). This supports the idea that the observed infrared luminosity is probably dominated by the AGN component, as estimated by Le Floc'h et al. (2007). In addition, one can note that the SFR derived on the basis of the [O II] line is significantly lower: $2 M_{\odot} \text{yr}^{-1}$ relying on the equivalent width and rest-frame absolute magnitude measured by Weiner et al. (2005) and the formula of Guzman et al. (1997), while we estimate $3.5 M_{\odot} \text{yr}^{-1}$ with an integration of [O II] of the spectra published by Le Floc'h et al. (2007) (see their figure 2a) and normalised to SDSS fluxes. This could be compatible with the IR-derived SFR only with a factor of extinction of 105 – 190, while $L_{\text{IR}}/L_{\text{B}} = 41$ if one assumes that only one third of the infrared luminosity contributes to the SFR. While a large scatter is known to affect [O II] luminosities as discussed by Weiner et al. (2007), the previous comparison stresses the importance of the actual fraction of the infrared luminosity due to the starburst: this fraction is often overestimated.

Acknowledgements. We thank the DEEP collaboration for providing us with the optical spectra of CFRS 14.1157. We are most grateful to C. Willmer and E. Le Floc'h, who help us in this procedure. This research has made use of the NASA/IPAC Extragalactic Database (NED), which is operated by the Jet Propulsion Laboratory, California Institute of Technology, under contract with the National Aeronautics and Space Administration.

References

- Alexander, D. M., Bauer, F. E., Chapman, S. C., Smail, I., Blain, A. W., Brandt, W. N., & Ivison, R. J. 2005, *ApJ*, 632, 736
- Becker, R. H., White, R. L., & Edwards, A. L. 1991, *ApJS*, 75, 1
- Becker, R. H., White, R. L., & Helfand, D. J. 1995, *ApJ*, 450, 559
- Braine J., Combes F. 1992, *A&A*, 264, 433
- Calzetti D., Armus L., Bohlin R. C., Kinney A. L., Koornneef J., Storchi-Bergmann T. 2000, *ApJ*, 533, 682
- Carilli, C. L., et al. 2005, *ApJ*, 618, 586
- Carilli, C. L., & Wang, R. 2006, *AJ*, 131, 2763
- Chilingarian I. 2002, Master thesis, Moscow State University, Faculty of Physics.
- Combes F., Maoli R., Omont A. 1999, *A&A*, 345, 369
- Condon, J. J., Anderson, M. L., & Helou, G. 1991, *ApJ*, 376, 95
- Condon, J. J. 1992, *ARA&A*, 30, 575
- Dahlen, T., Mobasher, B., Dickinson, M., Ferguson, H. C., Giavalisco, M., Kretchmer, C., & Ravindranath, S. 2007, *ApJ*, 654, 172
- Dale, D. A., et al. 2007, *ApJ*, 655, 863
- Devereux N., Taniguchi Y., Sanders D. B., Nakai N., Young J. S. 1994, *AJ*, 107, 2006
- Dey A., Graham J. R., Ivison R. J., Smail I., Wright G. S., Liu M. C. 1999, *ApJ*, 519, 610
- Douglas, J. N., Bash, F. N., Bozayan, F. A., Torrence, G. W., & Wolfe, C. 1996, *AJ*, 111, 1945
- Downes, D., & Eckart, A. 2007, *A&A*, 468, L57
- Elbaz, D., Cesarsky, C. J., Chanial, P., Aussel, H., Franceschini, A., Fadda, D., & Chary, R. R. 2002, *A&A*, 384, 848
- Evans, A. S., Solomon, P. M., Tacconi, L. J., Vavilkin, T., & Downes, D. 2006, *AJ*, 132, 2398
- Farrah, D., Afonso, J., Efstathiou, A., Rowan-Robinson, M., Fox, M., & Clements, D. 2003, *MNRAS*, 343, 585
- Flores, H., et al. 1999, *ApJ*, 517, 148
- Fomalont, E. B., Windhorst, R. A., Kristian, J. A., & Kellerman, K. I. 1991, *AJ*, 102, 1258
- Gao, Y., & Solomon, P. M. 2004, *ApJ*, 606, 271
- Genzel, R., & Cesarsky, C. J. 2000, *ARA&A*, 38, 761
- Gregory, P. C., & Condon, J. J. 1991, *ApJS*, 75, 1011
- Greve T. R. et al. 2005, *MNRAS*, 359, 1165
- Guzman, R., Gallego, J., Koo, D. C., Phillips, A. C., Lowenthal, J. D., Faber, S. M., Illingworth, G. D., & Vogt, N. P. 1997, *ApJ*, 489, 559
- Hammer, F., Crampton, D., Lilly, S. J., Le Fevre, O., & Kenet, T. 1995, *MNRAS*, 276, 1085
- Hammer, F., Flores, H., Elbaz, D., Zheng, X. Z., Liang, Y. C., & Cesarsky, C. 2005, *A&A*, 430, 115
- Kennicutt, R. C., Jr. 1998, *ApJ*, 498, 541
- Le Floc'h, E., et al. 2007, *ApJ*, 660, L65
- Lilly, S. J., Hammer, F., Le Fevre, O., & Crampton, D. 1995, *ApJ*, 455, 75
- Madau, P., Pozzetti, L., & Dickinson, M. 1998, *ApJ*, 498, 106
- Marzke, R. O., da Costa, L. N., Pellegrini, P. S., Willmer, C. N. A., & Geller, M. J. 1998, *ApJ*, 503, 617
- Mazzarella, J. M., Graham, J. R., Sanders, D. B., & Djorgovski, S. 1993, *ApJ*, 409, 170
- Melchior A.-L., Combes F., Guiderdoni B., Hatton S. 2001, ESA SP-460: The Promise of the Herschel Space Observatory, 467; preprint (astro-ph/0102086)
- Odehahn, S. C., & Aldering, G. 1995, *AJ*, 110, 2009
- Papadopoulos, P. P., Röttgering, H. J. A., van der Werf, P. P., Guilleaume, S., Omont, A., van Breugel, W. J. M., & Tilanus, R. P. J. 2000, *ApJ*, 528, 626
- Patnaik, A. R., Browne, I. W. A., Wilkinson, P. N., & Wrobel, J. M. 1992, *MNRAS*, 254, 655
- Sanders D. B., Scoville N. Z., Soifer B. T. 1991, *ApJ*, 370, 158
- Saripalli, L., & Mack, K.-H. 2007, *MNRAS*, 376, 1385
- Schmitt, H. R., Kinney, A. L., Calzetti, D., & Storchi Bergmann, T. 1997, *AJ*, 114, 592
- Seaquist, E. R., Ivison, R. J., & Hall, P. J. 1995, *MNRAS*, 276, 867
- Snellen, I. A. G., Lehnert, M. D., Bremer, M. N., & Schilizzi, R. T. 2002, *MNRAS*, 337, 981
- Solomon P. M., Downes D., Radford S. J. E., Barrett J. W. 1997, *ApJ*, 478, 144
- Solomon P. M., Vanden Bout P. A. 2005, *ARA&A*, 43, 677
- Spergel, D. N., et al. 2007, *ApJS*, 170, 377
- Steidel, C. C., Shapley, A. E., Pettini, M., Adelberger, K. L., Erb, D. K., Reddy, N. A., & Hunt, M. P. 2004, *ApJ*, 604, 534
- van den Bergh, S. 2001, *AJ*, 122, 621
- Vogt, N. P., et al. 2005, *ApJS*, 159, 41
- Vlahakis, C., Eales, S., & Dunne, L. 2007, *MNRAS*, 379, 1042
- Weiner, B. J., et al. 2005, *ApJ*, 620, 595
- Weiner, B. J., et al. 2007, *ApJ*, 660, L39
- White, R. L., & Becker, R. H. 1992, *ApJS*, 79, 331
- Wright, E. L. 2006, *PASP*, 118, 1711
- Yao, L., Seaquist, E. R., Kuno, N., & Dunne, L. 2003, *ApJ*, 588, 771
- Yun, M. S., Reddy, N. A., & Condon, J. J. 2001, *ApJ*, 554, 803
- Zheng, X. Z., Hammer, F., Flores, H., Assémat, F., & Pelat, D. 2004, *A&A*, 421, 847

Appendix A: CFRS 14.1329

This galaxy was first detected in radio by Fomalont et al. (1991). It was subsequently detected in the CFRS survey (Lilly et al., 1995; Hammer et al., 1995). It has been classified as a dusty Sa by van den Bergh (2001), while Flores et al. (1999) classified it as a strong starburst and highly reddened starburst with a lenticular morphology. Flores et al. (1999) fitted Schmitt et al. (1997) spectral energy distribution templates to optical, K and mid-infrared data, as well as to the $60\mu\text{m}$ flux (derived from the radio-FIR correlation). The infrared luminosity⁵ derived for CFRS 14.1329 in this way was $62.8 \pm 3.1 \times 10^{10} L_{\odot}$. We relied on this infrared luminosity to select CFRS 14.1329 for CO observations. In the meantime, Zheng et al. (2004) reanalysed a CFRS sample containing CFRS 14.1329 with the mid-infrared and infrared correlation found by Elbaz et al. (2002), and published a revised version of the infrared luminosity a factor of 4.8 smaller: $L_{\text{IR}} = 13.0 \pm 2.5 \times 10^{10} L_{\odot}$ ($\text{SFR} = 22.3 \pm 4.2 M_{\odot} \text{yr}^{-1}$).

⁵ This luminosity corresponds to $\text{SFR} = 107 \pm 5 M_{\odot} \text{yr}^{-1}$ relying on Kennicutt (1998).

⁴ Please note that Le Floc'h et al. (2007) worked with the $1-1000 \mu\text{m}$ range. In this paper, we adapted their figures to the $8-1000\mu\text{m}$ range used here, thanks to the corresponding value kindly provided by E. Le Floc'h.

This revision reflects the uncertainties related to the determination of the infrared luminosity based on correlations with other wavelengths luminosities. This lower value is in agreement with our non-CO detection (see Table 2). More recently, it has been further observed with the DEEP Groth Strip Survey (Vogt et al., 2005). In addition, Hammer et al. (2005) estimate $\text{SFR}([\text{O II}]) = 3.5 \text{ M}_{\odot} \text{ yr}^{-1}$, which would require a factor of extinction of 6.4, while $L_{\text{IR}}/L_B = 32.5$.

Appendix B: NGP9 F268-0341339

This object is a radio-flat spectrum galaxy. Its optical spectra is typical of an AGN. The SCANPI/IRAS tool suggests a possible signal at $12 \mu\text{m}$. However, there is foreground disc galaxy (SDSS J122847.72+370606.9) at $z = 0.138$, which is hosting an intense star formation activity ($\text{SFR} \sim 95 \text{ M}_{\odot} \text{ yr}^{-1}$). Its optical spectra is typical of an Sb galaxy, while it exhibits a strong H α emission line ($\text{SFR} \sim 95 \text{ M}_{\odot} \text{ yr}^{-1}$). Given its close angular distance ($5''$) to NGP9 F268-0341339, it most probably dominates the possible infrared IRAS fluxes.